Melting and Crystallization Behavior of Aliphatic Polyketones

G. A. HOLT, JR., J. E. SPRUIELL

Center for Materials Processing and Department of Materials Science and Engineering, University of Tennessee, Knoxville, Tennessee 37996-2200

Received 25 September 2000; accepted 16 April 2000

ABSTRACT: The basic crystallization and melting behavior of three aliphatic polyketones were studied using differential scanning calorimetry (DSC), wide-angle X-ray diffraction (WAXD), small-angle X-ray scattering (SAXS), and optical microscopy. One resin was a perfectly alternating copolymer of ethylene and carbon monoxide, while the other two resins were terpolymers in which 6 mol % propylene was substituted for ethylene. Small decreases in the melting point and percent crystallinity of these materials were displayed with repeated melting. This behavior was attributed to light crosslinking as a result of condensation reactions occurring at temperatures in the melting range. WAXS showed that, after cooling to room temperature, the crystalline form in the copolymer was the α-phase, while that in the terpolymers was the β-phase. Optical microscopy revealed that the materials produce both negative and mixed birefringence spherulites under the conditions studied. SAXS measurements showed that the lamella thickness was largely a function of the temperature of crystallization. Attempts were made to measure the equilibrium melting temperature of these resins using several available techniques. The best value of the equilibrium melting temperature was concluded to be 278 $\pm$ 2°C for the copolymer. The results varied over a wide range for the terpolymers, but it is suggested that appropriate values are of order 252°C for the terpolymers. Crystallization kinetics studies, carried out under isothermal conditions using DSC, were evaluated using the Avrami equation. Results showed the Avrami exponent to lie in the range of 2–3. Spherulite growth rates were interpreted in terms of the secondary nucleation theory of Lauritzen and Hoffman. A transition from regime II to regime III was discovered. J Appl Polym Sci 83: 2124–2142, 2002

Key words: aliphatic polyketones; melting point; crystallization; DSC; SAXS

INTRODUCTION

Aliphatic polyketone resins were first synthesized and studied by Brubaker et al.[1] in 1952, and they have been discussed in terms of thermolysis, photochemistry, and synthesis by several early investigators.[2–6] These copolymers of carbon monoxide and olefins were of interest for many years, but with certain synthesis and stability limitations, their chance of becoming commercialized was not very promising. These problems have been largely overcome and a family of aliphatic polyketones (terpolymers of ethylene and propylene with carbon monoxide) were recently developed. These resins display a balance of toughness, stiffness, chemical resistance, and ease of processing that make them good prospects for several appli-

Correspondence to: J. E. Spruiell.
Contract grant sponsor: Shell Chemical Co.

Journal of Applied Polymer Science, Vol. 83, 2124–2142 (2002)

DOI 10.1002/app.10165

cations (such as in the appliance, automotive, and electrical industries). Thus, it is important to understand the structure, properties, advantages, and limitations of these materials.

The molecular and crystal structure and melting behavior of the perfectly alternating ethylene and carbon monoxide (polyketone) copolymer was earlier studied using H-nuclear magnetic resonance, thermal analysis, and X-ray diffraction.[7–12] Lommerts also studied fiber formation in the perfectly alternating ethylene–carbon monoxide copolymer using a solution spinning technique.[11] The effect on the structure and phase stability of substituting propylene for part of the ethylene during the synthesis of the polymer was described by Lommerts[11] and Klop et al.[12] Later, a series of articles emphasizing the physical and chemical characteristics of the terpolymers was published. This series included a brief presentation of the (1) synthesis and stability of the resins[13]; (2) thermal properties, morphology, and isothermal crystallization behavior[14]; rheological and melt-processing behavior[15]; and chemical resistance and barrier properties.[16]

In the present research, the basic crystallization and melting behavior, the isothermal crystallization kinetics, and the structure of aliphatic polyketones were further investigated using several techniques. These include

1. Differential scanning calorimetry (DSC), used to investigate the melting and crystallization under nonisothermal conditions and to measure the isothermal crystallization kinetics.
2. Wide-angle X-ray diffraction (WAXD), used to investigate the crystal phase(s) present for each material after a given treatment.
3. Small-angle X-ray scattering (SAXS), used to determine the long period and lamellar thickness as a function of the crystallization temperature.
4. Optical microscopy, used to evaluate the spherulite birefringence and to obtain spherulite linear growth rate data for these materials.

EXPERIMENTAL

Materials

The Shell Chemical Co. (Houston, TX) supplied the polymers used in this study, in pellet form. There were three grades:

1. A copolymer: a general-purpose copolymer of perfectly alternating carbon monoxide and ethylene with a weight-average molecular weight of approximately 40,000 and a polydispersity index of 3.09.
2. A high molecular weight (HMW) terpolymer: a general-purpose terpolymer which has propylene (≈6 mol %) substituted randomly for ethylene and alternately with carbon monoxide with a weight-average molecular weight of approximately 80,000 and a polydispersity index of 2.99.
3. A low molecular weight (LMW) terpolymer: a terpolymer of similar composition with a weight-average molecular weight of approximately 40,000 and a polydispersity index of 2.32.

Technique and Sample Preparation

Differential Scanning Calorimetry (DSC)

DSC was used to investigate the melting and crystallization behavior under constant heating and/or cooling rates. It was also used to study the isothermal crystallization kinetics of the aliphatic polyketone resins. To prevent thermal oxidative degradation of the materials, the experiments were carried out using a Perkin–Elmer series 7 differential scanning calorimeter with a blanket of nitrogen gas. The instrument was calibrated using the melting onset and heat of fusion of indium as a standard (T_m = 156.5°C, ΔH_f = 28.5 J/g). The DSC samples were cut from pressed films and placed in aluminum sample pans. The films were prepared by first drying the materials at 60°C for 6–8 h. Next, the materials were pressed into film sheets using a Wabash 12-ton melt press. The pellets were placed between two clean sheets of Kapton film, which, in turn, were placed between two stainless-steel platens. The platens were then positioned between the preheated plates of the press. The terpolymer samples were pressed at 250°C, and the copolymer was pressed at 275°C. The polymer pellets were allowed to melt for approximately 2 min and then pressed with an applied pressure of about 2 ton/in.^{2} for 2 min. After this process, the film was allowed to cool to room temperature. Several films were prepared for each material.

For the melting and crystallization of the copolymer, the samples were heated to 275°C at a scanning speed of 20°C/min and held at that temperature for 3 min to remove the effects of prior

deformation and the thermal history. Then, the sample was cooled at the same rate. After crystallization, the sample was reheated and melted again. The same procedure was used for the terpolymers except that the melt-holding temperature was 250°C.

For the isothermal crystallization kinetics studies, the copolymer sample was heated to 275°C (or 250°C for the terpolymers) at a scanning speed of 20°C/min and held at that temperature for 3 min, to remove the effects of prior deformation and the thermal history. Then, the sample was cooled to the desired crystallization temperature (T_c) at a rate of 200°C/min. The sample was held at this temperature for 5–20 min, depending on the crystallization temperature chosen (higher T_c, longer hold time). Then, to observe the resulting melting temperature, the sample was melted again.

X-ray Analysis

1. WAXD diffractometer patterns were obtained, in reflection, using a Rigaku Denki diffractometer and CuKα radiation. Samples were prepared by melting pellets into a film approximately 0.5 mm thick. They were prepared under a nitrogen atmosphere to minimize degradation using a Mettler FP 82 hot stage calibrated to $\pm$0.5°C. The copolymer was melted and held at 275°C for 3 min before cooling rapidly to the desired crystallization temperature. The terpolymer samples were prepared in the same way except that they were melted and held at 250°C for 3 min before cooling to the crystallization temperature.
2. SAXS studies were conducted at the Oak Ridge National Laboratories, Center for Small Angle Scattering Research in Oak Ridge, TN.[17] The apparatus has pinhole geometry, a rotating anode CuKα X-ray source, a two-dimensional position-sensitive detector, and a sample-to-detector distance of 5.12 m. The scattering intensity was stored in a 64 $\times$ 64 data array. Corrections were made for the instrumental background, dark current due to cosmic radiation, electronic noise, and detector nonuniform sensitivity. The intensity data were azimuthally averaged and converted to the absolute differential cross section using precalibrated secondary standards. The same samples used in the WAXD experiments were used for the SAXS studies.

Density Crystallinity

Density values were measured using a density-gradient column prepared from sodium bromide and water. Percent crystallinity was computed assuming a two-phase model in the usual way. In this calculation, the value for the density of the different phases were taken as follows: 1.382 g/cm^3 for the α-phase, 1.297 g/cm^3 for the β-phase, and 1.21 g/cm^3 for the amorphous phase.

Optical Microscopy

Isothermal spherulitic growth rates for the three aliphatic polyketones were measured using optical microscopy. The growth-rate experiments were carried out by video recording the crystallization process at each crystallization temperature. After each run, several spherulite diameters were measured as a function of time. The values for the different spherulites were averaged. The samples for these studies were prepared in the same manner as were the samples for the X-ray analysis except that these samples had a thickness of approximately 150 μm. Polarized light microscopy was also used to classify the spherulites of these materials on the basis of the sign of their birefringence.

RESULTS AND DISCUSSION

Preliminary Nonisothermal Melting and Crystallization Behavior

Examples of DSC melting endotherms after each of three successive heating and cooling cycles (20°C per minute) are presented in Figure 1 for the HMW terpolymer. The melting temperature of this sample is observed to decrease with every melting–cooling cycle. Similar behavior was also found for the other two resins. The peak melting temperatures after one to three thermal cycles are summarized in Table I. Decreases of T_m from 255 to 251°C for the copolymer and from 226 to 222°C for the terpolymers were observed after three cycles. The observed peak crystallization temperature, after each thermal cycle, is given in Table II. The peak crystallization temperature decreases after each melting cycle for all three polymers.

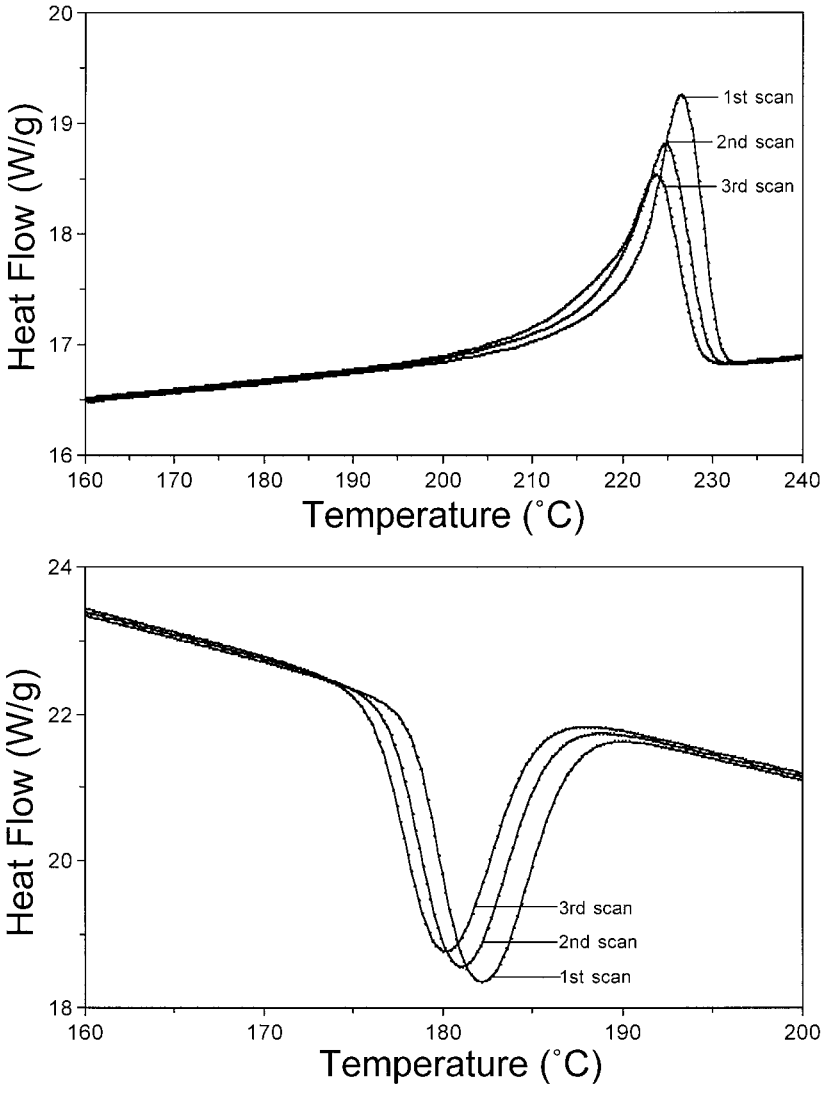

Figure 1 Typical DSC melting and cooling scans for the HMW terpolymer.

The measured heats of fusion of the materials were also found to decrease with every melting–cooling cycle as shown in Table III. A decrease in the measured ΔH from about 116 to 99 J/g for the copolymer was observed between the first and third thermal cycle. For the HMW terpolymer, the decrease was from 71 to 67 J/g, and for the LMW terpolymer, it was from 85 to 77 J/g.

The observed melting behavior in the co- and terpolymers is likely due to condensation reactions that occur at temperatures in the melt-holding range.[13,15] These reactions lead to crosslink-

Table I Peak Melting Temperature After Each of Three Thermal Cycles

Material	T_m (One Cycle)	T_m (Two Cycles)	T_m (Three Cycles)
HMW terpolymer	226.3°C	223.7°C	223.4°C
LMW terpolymer	225.0°C	223.7°C	222.7°C
Copolymer	255.5°C	253.2°C	251.1°C

Table II Peak Crystallization Temperatures After Each of Three Thermal Cycles

Material	T_c (One Cycle)	T_c (Two Cycles)	T_c (Three Cycles)
HMW terpolymer	182.2°C	180.9°C	180.0°C
LMW terpolymer	188.7°C	187.5°C	186.6°C
Copolymer	214.9°C	212.9°C	211.1°C

ing of the polymer chains. The crosslinks interfere with the crystallization process on subsequent cooling, resulting in a lowering of the crystallization temperature (Table II) and a decrease in the crystallinity and/or perfection of the crystals formed; the latter results in a decrease in the heat of fusion on subsequent melting (Table III). It is well established that the melting temperature of a polymer is affected by the temperature at which it was crystallized, due to the influence of crystallization temperature on the lamellae thickness. This would explain the lower melting temperature after each cycle, as shown in Table I.

Phase Structure

WAXD (diffractometer) patterns were used to ascertain the phase structure for samples crystallized at a series of crystallization temperatures covering the range of temperatures at which isothermal crystallization could be carried out. Previous research has shown that two crystal forms exist in these aliphatic polyketones. An α-form was reported by Lommerts et al.[7,11] in well-oriented fibers of the perfectly alternating copolymer. This form is orthorhombic, space group *Pbnm*, with $a = 0.691$ nm, $b = 0.512$ nm, and $c = 0.760$ nm (chain axis). A β-form was reported earlier by Chatani et al.[10] The β-form is also orthorhombic, space group *Pnam* with $a = 0.797$ nm, $b = 0.476$ nm, and $c = 0.757$ nm. The α-phase is more compact with a density of 1.382 g/cm^3 compared to a density of 1.297 g/cm^3 for the β-phase. According to Flood et al.,[14] both unit cells may coexist in both the copolymer and in the terpolymers; the relative amount of each phase present is dependent on the thermal history, orientation level, and termonomer content. Lommerts[11] and Klop et al.[12] showed that the α-phase was the dominant one in the copolymer at room temperature. They showed that the copolymer undergoes a reversible transition between 110–130°C from the α-phase to the β-phase. Further, the incorporation of propylene–carbon monoxide segments into the chain inhibits the formation of the α-phase in oriented fibers. At compositions above 5 mol % of such segments, no α-phase was found in the terpolymer fibers. This would suggest that only the β-phase would be expected for the present terpolymers after crystallization.

Room-temperature WAXD diffractometer patterns were run on samples crystallized at different temperatures in the temperature range studied in this article. Figure 2 shows an example of the results for the copolymer and the HMW terpolymer, while Table IV lists the d-spacings and relative intensities of the diffraction peaks present in the patterns. According to the calculated diffraction patterns of the α- and β-phases presented by Klop et al.[12] (see comparison in Table IV), the HMW terpolymer is largely β-phase and the copolymer is largely α-phase at room temperature. Samples crystallized at all temperatures studied exhibited diffraction patterns that were virtually identical to those shown in Figure 2. Likewise, the samples of the LMW terpolymer

Table III Heats of Fusion (ΔH) After Each of Three Thermal Cycles

Material	ΔH (One Cycle)	ΔH (Two Cycles)	ΔH (Three Cycles)
HMW terpolymer	70.61J/g	69.10J/g	67.33J/g
LMW terpolymer	84.63J/g	79.54J/g	77.42J/g
Copolymer	115.57J/g	105.31J/g	98.91J/g

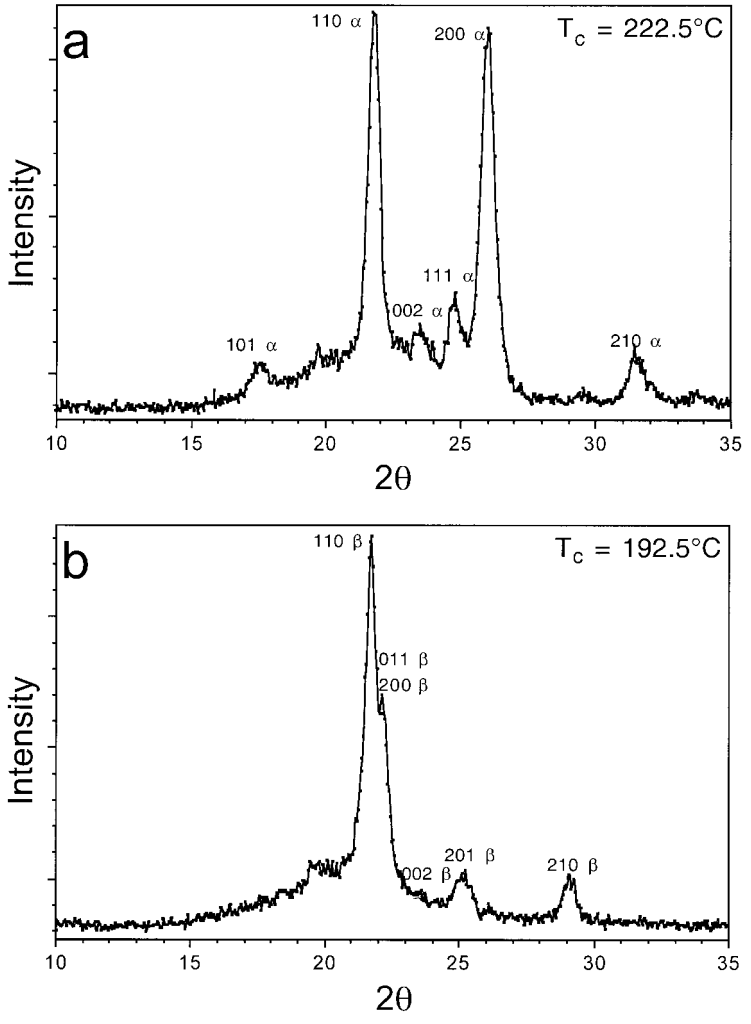

Figure 2 WAXD patterns for the (a) copolymer and (b) HMW terpolymer.

exhibited patterns that were quite similar to those of the HMW terpolymer, indicating that the predominant crystalline form in them was the β-phase.

It is important to note that the α-phase present in the copolymer was formed on cooling from the crystallization temperature, as all crystallization temperatures for the copolymer were well above the temperature at which the reversible transition from the α- to the β-phase was observed by Klop et al.[12] We also observed substantial quantities of the β-phase in the copolymer when cooled rapidly from the crystallization temperature. Thus, we conclude that crystallization under the conditions studied in this article resulted in the formation of the β-phase directly from the melt for both the terpolymers and the copolymer. Similarly, the heat of fusion measured when either the copolymer or the terpolymer was melted at reasonable heating rates represents the melting of the β-phase.

Morphology

In the past, the morphology of the terpolymer was described as an "entangled" spherulitic structure, and the copolymer, as an "entangled" hedritic structure[14] (on the 5–50-μm level). These observations were performed using optical photomicrographs and environmental scanning electron microscopy (ESEM). When viewed through crossed polars, spherulites show a characteristic isogyral cross (Maltese cross) with wings coinciding with the respective planes of the polarizer and the analyzer. Spherulites can be optically positive or negative, depending on their birefringence.[18] The birefringence of a spherulite, Δ_s, is defined as $n_r -$

Table IV X-Ray Diffractometer Results for the HMW Terpolymer and Copolymer

Material	Observed 2θ	Measured d-Spacing (nm)	Observed Intensity	Literature Values for d-Spacing (nm)	Miller Indices	Literature Intensity	Crystal Phase
HMW terpolymer	21.8	0.408	Very strong	0.408	110	Very strong	β
	22.3	0.402	Strong	0.403	011	Medium	β
	22.4	0.397	Strong	0.397	200	Strong	β
	23.5	0.379	Very weak	0.380	002	Very weak	β
	25.2	0.353	Weak	0.353	201	Weak	β
	29.2	0.306	Medium	0.306	210	Medium	β
	37.8	0.238	Very weak	0.238	212	Very weak	β
	—	—	—	0.232	310	Very weak	β
	40.2	0.223	Weak	0.224	013	Weak	β
	42.2	0.214	Very weak	0.213	203	Very weak	β
Copolymer	17.5	0.507	Medium	0.507	101	Medium	α
	21.7	0.410	Strong	0.408	110	Strong	α
	23.5	0.379	Very weak	0.379	002	Very weak	α
	24.8	0.359	Medium	0.359	111	Medium	α
	25.9	0.344	Strong	0.344	200	Strong	α
	29.3	0.305	Very very weak	0.306	210	Medium	β
	31.3	0.286	Medium	0.286	210	Medium	α
	42.0	0.215	Medium	0.216	301	Medium	α

n_t, where n_r is the refractive index parallel to the spherulite radius, and n_t, the refractive index perpendicular to the radial direction (tangential to the spherulite). Thus, a spherulite with negative birefringence has a greater index of refraction in the tangential direction and a spherulite with positive birefringence has a greater index of refraction in the radial direction.

The sign of birefringence of the spherulite can be determined using a primary red filter (λ-plate) located diagonally between crossed polars. When a spherulite is negative, its first and third quadrants are yellow and the second and fourth ones are blue, while for a positive spherulite, the first and third quadrants are blue and the second and fourth ones are yellow.[19]

Photomicrographs of the terpolymer and copolymer materials show that negative and mixed birefringence spherulites are present in these polyketones. The negative spherulites indicate that the polymer chains tend to be aligned in the tangential direction while the mixed spherulites suggest that there may be two or more crystallite orientations in the spherulite.[19] The terpolymer materials seem to have a higher number of the negative spherulites than has the copolymer; the latter has an approximately equal number of the negative and mixed spherulites. The aliphatic polyketones display similar micrographs at each investigated isothermal temperature. No noticeable difference in the types of spherulites present was observed with respect to crystallization temperature for any of the materials.

Long-period spacings were measured by SAXS at selected crystallization temperatures. Initially, the SAXS data was collected as circular-shaped two-dimensional intensity plots, then azimuthally averaged and plotted as the intensity versus the scattering vector Q. Since Q_{max} is needed to determine the long period (L), the Lorentz correction or Kratky plot (Q^2I versus Q) is used to better identify Q_{max} from the SAXS data. Figure 3 shows an example of the Lorentz-corrected data of a few samples of the copolymer crystallized at different crystallization temperatures.

The values of the long periods for selected crystallization temperatures are presented in Table V. Note that the long period increases with the crystallization temperature for all three resins. The values for the two terpolymers are very similar at equivalent crystallization temperatures, with the LMW terpolymer tending to have a slightly smaller long period. Note that the range of crystallization temperatures is fairly re-

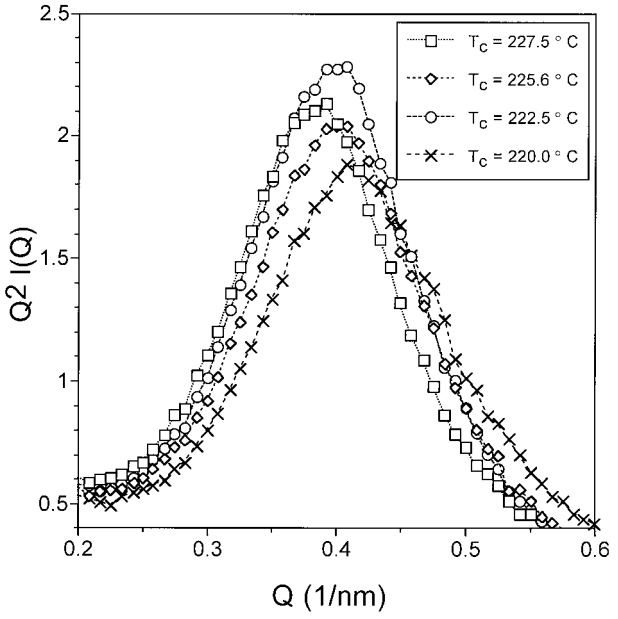

Figure 3 Selected Lorentz-corrected SAXS data for the copolymer.

stricted. The lowest crystallization temperature for each resin was determined by the necessity of reaching thermal equilibrium at the crystallization temperature before the onset of crystallization; the highest crystallization temperature was required to be low enough to avoid appreciable degradation or crosslinking before the completion of the crystallization process. This temperature range was quite different for the copolymer compared to the terpolymers. Since the melting temperature of the copolymer is higher than that of the terpolymers, the lowest crystallization temperature for the copolymer was higher than was the crystallization temperature for the terpolymers. On the other hand, the crystallization rate of the copolymer was fast enough that the polymer could be crystallized at much higher temperatures than could the terpolymers without appreciable degradation or crosslinking. The temperature range in which experiments could be appropriately carried out is quite important as it influences much of what follows.

The density crystallinity (volume fraction) of the samples whose long period was measured is also given in Table V. The crystallinity of the copolymer was substantially higher than that of the terpolymers at all conditions studied, as expected. The values for the two terpolymers were quite similar. The values tended to increase slightly with increase in the temperature for all three resins.

Values of the crystal lamellae thickness, l_c , were computed by multiplying the long-period values by the volume-fraction crystallinity as determined from the density measurements. The resulting lamellae thickness values are plotted in Figure 4. For each resin, the lamellae thickness increases with an increasing crystallization temperature. Two linear lines are shown in Figure 4. The dot–dash line represents a best linear curve fit to the data for the copolymer. Note that the extension of this curve is near, but slightly below the bulk of the terpolymer data. The dashed line represents a trend line that was selected to give a reasonable fit to all the data. This line differs only slightly from the dot–dash line in the range where the copolymer data exist. This suggests that the crystallization temperature largely controls the lamellae morphology developed in these resins independent of the resin composition. The influence of the terpolymer is to lower the melting temperature and the temperature range in which crystallization can be studied.

Estimation of Heat of Fusion and Equilibrium Melting Temperature

A full interpretation of the crystallization kinetics of a polymer requires knowledge of its heat of

Table V Long Period Spacings and Density Crystallinity Values

Material	T_c (°C)	Long Period (nm)	Volume Fraction Crystalline
HMW terpolymer	200.0	18.04	46.2
	195.0	17.79	43.1
	192.5	17.43	41.8
	190.0	17.45	41.6
	187.0	16.51	41.0
	182.5	15.64	40.8
LMW terpolymer	200.0	17.55	46.1
	197.5	17.75	44.3
	192.5	16.25	43.3
	190.0	16.47	39.6
	187.0	14.96	41.8
Copolymer	227.5	16.84	66.6
	225.6	16.01	65.6
	222.5	16.17	66.9
	220.0	15.35	66.0
	217.5	15.37	65.5
	212.5	14.81	63.2

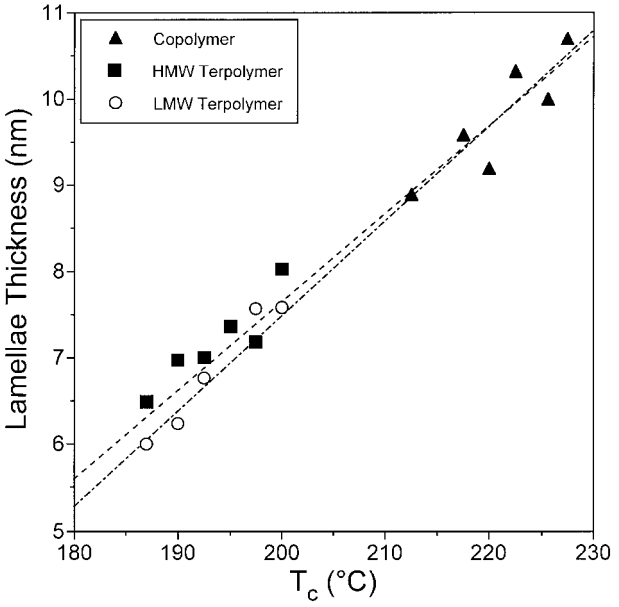

Figure 4 Lamellae thickness versus crystallization temperature for the three resins.

fusion per gram of crystal and its equilibrium melting temperature. Further, these quantities are very important thermal properties of any polymer. Since both the heat of fusion and the equilibrium melting temperature were not accurately known for these aliphatic polyketones, we carried out several experiments in an effort to obtain reasonable values for these parameters for the three resins studied here.

Based on melting data for a series of low molecular weight polyketone homologs, Lommerts et al.[7] estimated that the heat of fusion for a high molecular weight copolymer sample was in the range 215–330 J/g. Later, Flood et al.[14] quoted a value of 227 J/g, based on data obtained by other Shell investigators. It is believed that this value also was obtained from thermodynamic data on low molecular weight homologs. In the discussion of Flood et al., no distinction was made between the values for the copolymer and the terpolymers.

We combined density crystallinity and heat of fusion measurements for a series of samples to estimate the heat of fusion per gram of crystal (i.e., for 100% crystalline material). This approach requires the value of the density of both the crystalline and amorphous phases and assumes a two-phase structure of the samples. Based on the X-ray data described above, it was assumed that the crystalline phase in the samples (at room temperature) was the α-form for the copolymer and the β-form for the terpolymers. The crystalline densities used were those calculated from the X-ray data (1.382 g/cm^3 for the α-phase and 1.297 g/cm^3 for the α-phase). Lommerts et al.[7] gave a value of 1.21 g/cm^3 for the amorphous density, although it is not clear how it was obtained. We extrapolated to room temperature (25°C) data for the specific volume of the melt as a function of temperature to estimate the density of the amorphous phase. This extrapolation gave a value of 1.205 g/cm^3. Based on these results, we accepted the value of 1.21 g/cm^3 suggested by Lommerts et al. Using these values, our results for a series of samples produced values of 226 $\pm$ 16 J/g for the heat of fusion per gram of crystal for the terpolymer materials and 239 $\pm$ 11 J/g for the copolymer material. The value for the terpolymer materials is almost the same as the value quoted by Flood et al., while the copolymer value is slightly higher. The observed differences between the copolymer and the terpolymers do not appear to be statistically significant in view of the quoted error. Nevertheless, our result is in line with expectations if one assumes that the terpolymer crystals may contain a higher defect content than that of the copolymer.

We attempted to determine the equilibrium melting temperatures by techniques that are described in the literature. This process is fraught with numerous difficulties for any polymer, but especially for the present resins. To begin with, the data in Table I showed that with increased thermal exposure the melting temperatures decrease. This indicates that the equilibrium melting temperature is likely to be a function of the thermal history or, more precisely, the level of crosslinking in the sample. Furthermore, crosslinking (along with the change in the melting temperature) increases as the crystallization temperature increases due to the faster reaction rates and longer exposures required for crystallizing the samples. The techniques used to determine the equilibrium melting temperature require that the samples have different thermal histories and, therefore, slightly different levels of crosslinking. Thus, the temperature range for crystallization experiments must be restricted to a range where the effects of crosslinking are deemed to be negligible.

In addition to these special problems for the present resins, there is no general agreement in the literature regarding the best way to determine the equilibrium melting temperature. The two most commonly used techniques are (1) the Hoffman–Weeks method[20] and (2) the use of the

Gibbs–Thomson equation.[21] Both of these techniques involve assumptions that are not universally valid, as was recently discussed by Marand et al.[22,23] and others.[24,25]

The Gibbs–Thomson equation reads

$$T_m = T_m^0 - \frac{2\sigma_e T_m^0}{l_c \Delta H_f} \quad (1)$$

where σ_e is the fold surface free energy; l_c, the lamellae thickness; and ΔH_f, the heat of fusion of the crystal. According to eq. (1), the equilibrium melting temperature, T_m^0, is given as the intercept of a plot of the measured melting temperature, T_m, versus the reciprocal lamellae thickness ($1/l_c$). The fold surface free energy can be calculated from the slope of this plot provided that the heat of fusion is known. In the derivation of the Gibbs–Thomson equation, it is assumed that the energy associated with the lateral (side) surfaces of the crystal lamellae is negligible compared to that of the fold surfaces. This will be true if the crystal dimensions perpendicular to the thickness direction are large relative to the crystal thickness and/or the fold surface free energy is large compared to the lateral surface free energy. We expect this to be the case for the present polymers.

The Hoffman–Weeks method obtains the equilibrium melting temperature of a polymer from a plot of the measured melting temperature, T_m, versus the temperature at which the sample was crystallized, T_c, and extrapolating the data to the line corresponding to $T_m = T_c$ (the Hoffman–Weeks plot).[20] In addition to the assumptions involved in the Gibbs–Thomson analysis, the Hoffman–Weeks method depends on the assumption that the difference between the crystallization temperature and the melting temperature is due to the thickening of crystals formed at the crystallization temperature. If a constant thickening coefficient, β, is assumed, the relation between the melting and crystallization temperatures is linear, and the equilibrium melting temperature corresponds to the extrapolated temperature where $T_m = T_c$. Unfortunately, as pointed out by Alamo et al.,[24] plots of T_m versus T_c are not always linear when plotted over a wide range of crystallization temperatures. This can lead to substantial error in the estimated equilibrium melting temperature if a linear relation is assumed for data obtained over a narrow crystallization temperature range. Marand et al.[22] developed a more rigorous relationship between the observed melting and crystallization temperatures that explains the curvature in such plots. Based on this relationship, they suggested a new method of obtaining the equilibrium melting temperature from such data, referred to as the nonlinear Hoffman–Weeks analysis (NLHW). Their analysis showed that the original Hoffman–Weeks method typically underestimates the equilibrium melting temperature and overestimates the thickening coefficient. The new NLHW analysis involves plotting $T_m^0/(T_m^0 - T_m)$ versus $T_m^0/(T_m^0 - T_c)$. For the true equilibrium melting temperature, such a plot is linear with the slope equal to the thickening coefficient. They concluded that this approach provides an acceptable value of the equilibrium melting temperature when (a) the thickening coefficient is constant and substantially greater than unity or (b) the thickening coefficient is known to be unity (see ref. 22 for more detail). Unfortunately, these are fairly restrictive conditions that may not often be met in practice.

Finally, as pointed out by Huang et al.[26] and Xu et al.,[23] it is possible to obtain the equilibrium melting temperature from the spherulitic growth rate data. This is done by achieving the smallest variance of the fit of the growth rate data to the Hoffman–Lauritzen equation by varying the equilibrium melting temperature used in the analysis. If a regime transition is present, the procedure involves choosing the equilibrium melting temperature so as to obtain a value of 2.0 for the ratio of the two secondary nucleation constants. This method obviously assumes that the growth rates can be described in terms of the Hoffman–Lauritzen equation.

We attempted to obtain the equilibrium melting temperatures of the present resins by each of the above techniques. Our results and a further discussion of them are described below, beginning with the Gibbs–Thomson analysis.

Figure 5 shows the T_m versus $1/l_c$ plot for all three materials using density data to obtain the crystalline volume fraction used in the calculation of the lamellae thickness. To minimize the degree of crosslinking, we used a fresh sample for each crystallization temperature. Further, the crystallization temperatures were limited to a range below which there was little degradation and/or crosslinking and above which isothermal conditions can be achieved. While this was deemed necessary, it also limits the crystal size range present in the crystallized samples and limits the

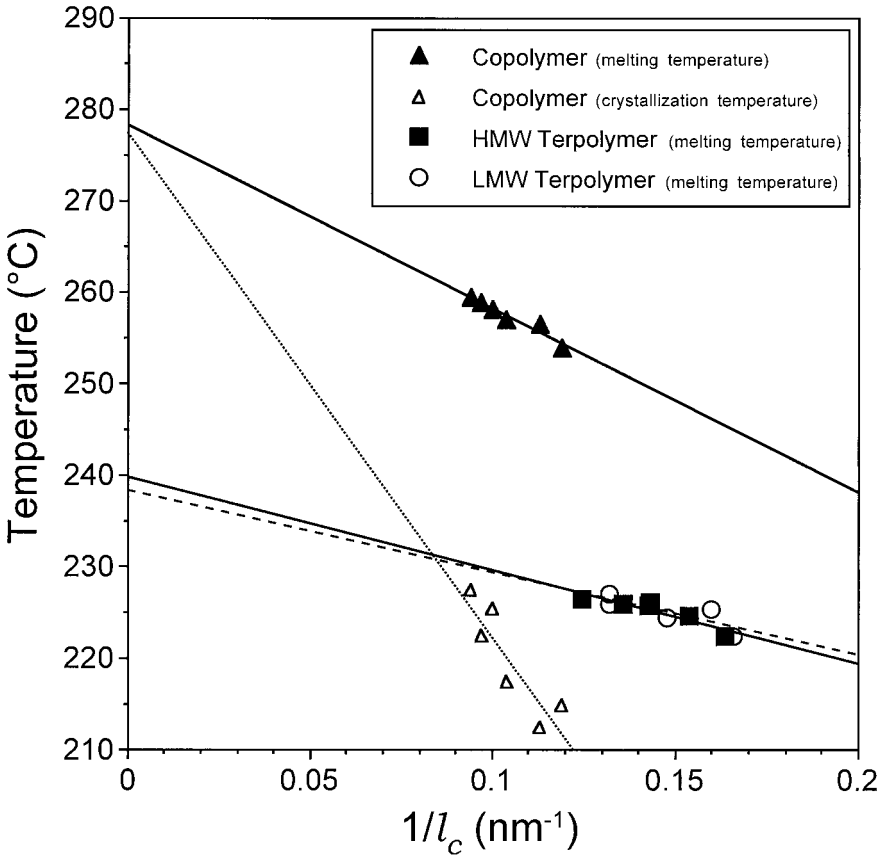

Figure 5 Relationship among the reciprocal lamellae thickness, the crystallization temperature for the copolymer, and the melting temperature for the three resins.

temperature range in which data are available for plots such as those shown in Figure 5. The value of the equilibrium melting temperature for the copolymer obtained from the Gibbs–Thomson analysis compares quite favorably with a value of 278°C suggested by Lommerts et al.[7] for a perfectly alternating copolymer based on the observed melting points of highly oriented fibers produced by gel spinning and drawing. A linear plot of the crystallization temperature, T_c, versus the reciprocal lamella thickness for the copolymer is also given in Figure 5. Although there is not a firm theoretical foundation for such a plot, it has been suggested that such a linear curve should intersect the Gibbs–Thomson extrapolation at the equilibrium melting temperature since, at this point, $T_m = T_c$. We would further anticipate that the intersection should occur at the reciprocal lamella thickness equal to zero (infinite lamella thickness). The observed intercept at infinite lamella thickness of 277.5°C is in good agreement with the value of 278°C obtained from the Gibbs–Thomson extrapolation.

Before considering the Gibbs–Thomson results for the terpolymers, it is important to note that the perfectly alternating copolymer could also be considered a homopolymer in which the monomer is —(CH_2—CH_2—CO)—. Thus, we see no reason why the Gibbs—Thomson analysis cannot be used to obtain the equilibrium melting temperature of the perfectly alternating copolymer. But, in this context, the terpolymers must be considered as random copolymers with the chemical formula —(CH_2—CH_2—CO)$_n$—(CH_2—CH(CH_3)—CO)$_m$—.

As a first approximation, we may estimate the depression of the equilibrium melting temperature of the terpolymers compared to the copolymer from the Flory–Huggins expression.[27,28] With the assumption that we have A units that crystallize and B units that do not (the propylene units) and that the latter are distributed at random, this reads

$$\frac{1}{T^0_{\text{ter}}} - \frac{1}{T^0_{\text{co}}} = -\frac{R}{\Delta H_u} \ln X_A \qquad (2)$$

where T^0_{ter} is the equilibrium melting temperature of the terpolymer; T^0_{co}, the melting temperature of the copolymer; ΔH_u, the heat of fusion; and X_A, the mol fraction of propylene units. Assuming 278°C for the equilibrium melting temperature of the copolymer and 6 mol percent propylene units, eq. (2) yields 266°C as the equilibrium melting temperature of the terpolymer. This value is substantially higher than are the values of 240°C for the HMW terpolymer and 238°C for the LMW terpolymer obtained from the Gibbs–Thomson extrapolation. In the case of the terpolymers, the crystallite thickness and melting temperature may be affected by the longest sequence of crystallizable units as well as by the crystallization temperature. If this were the case, the Gibbs–Thomson equation would not rigorously apply to the terpolymers.[22,24] Consequently, we must use caution in interpreting the Gibbs–Thomson plots for the terpolymers, although the data plotted in Figure 4 suggest that the lamella thickness values for the terpolymers are largely controlled by the temperature. If the crystal thickness values are controlled by the sequence distribution of noncrystallizable units, we would expect the Gibbs–Thomson extrapolation to give a value that is too low. One should keep in mind that the error caused by differences in the thermal history for the samples would tend to reduce the melting point of samples exposed to greater thermal history. Consequently, we would expect this error would tend to produce equilibrium melting temperatures that are a bit low for both the copolymer and the terpolymer samples.

We crystallized samples of all three resins isothermally at a series of temperatures and then immediately melted them. A plot of the melting temperature versus the isothermal crystallization temperature is shown in Figure 6. Application of the original (linear) Hoffman–Weeks analysis to these data results in equilibrium melting temperatures of 272°C for the copolymer, 244°C for the HMW terpolymer, and 243°C for the LMW terpolymer. Note, however, that the difference between the latter two values is probably not statistically significant. Comparing the results derived from the Gibbs–Thomson plot to those derived from the Hoffman–Weeks plot, we observe that the value of $T_m{}^0$ derived from the Hoffman–Weeks plot for the copolymer is lower than is the value obtained from the Gibbs–Thomson analysis, while the values obtained for the terpolymers are slightly higher. Many of the same sources of error and problems with the analysis of the terpolymer data described above for the Gibbs–Thomson analysis also exist for the Hoffman–Weeks analysis. Further, we note that the NLHW analysis of Marand et al. suggests that the values obtained from the linear Hoffman–Weeks analysis are systematically low. Thus, these values are likely somewhat low.

To apply the NLHW analysis, we must *a priori* know the value of the lamella-thickening coefficient, β, or it should be large.[22] In the present case, we have no *a prior* idea what the value of β should be, and our attempts to establish it from the data according to the procedure of Marand et al.[22] failed to give definitive values for β. Thus, the best that we could do in this case was to assume values of β and then determine the corresponding values of the equilibrium melting temperature. With the assumption that the thickening coefficient is unity (nonthickening), this procedure gave values of 297.4°C for the copolymer, 275°C for the HMW terpolymer, and 273°C for the LMW terpolymer. On the other hand, assuming that the thickening coefficient is equal to 2.0 gives a value of 279.6°C for the copolymer. It is noteworthy that the latter value is in reasonable agreement with the value obtained from the Gibbs–Thomson analysis. The values obtained for the terpolymers with β equal to 2.0 are 250.3°C for the HMW terpolymer and 249.5°C for the LMW terpolymer.

If we use the technique[23,26] for determining the equilibrium melting temperature from the spherulite growth rate data (we will discuss our linear growth rate data in detail later in this article), we obtain a value of 280°C for the copolymer, in excellent agreement with the result from the Gibbs–Thomson analysis. This is consistent with a value of the thickening coefficient of about 2.0, if the NLHW approach is used. Thus, we believe that all the results for the copolymer are reasonably consistent with an equilibrium melting temperature of 278 $\pm$ 2°C, and we will use this value in further treatment of our data. The values produced by this technique for the terpolymers are 252.5°C for the HMW terpolymer and 246°C for the LMW terpolymer. The value for the LMW terpolymer is more than likely low due to the fact that more spherulite growth rate data are needed in the regime II domain. Clearly, the values obtained from the various techniques for the terpolymer differ substantially and there is no clear way to decide which value is best. We believe that the value should be greater than that obtained from

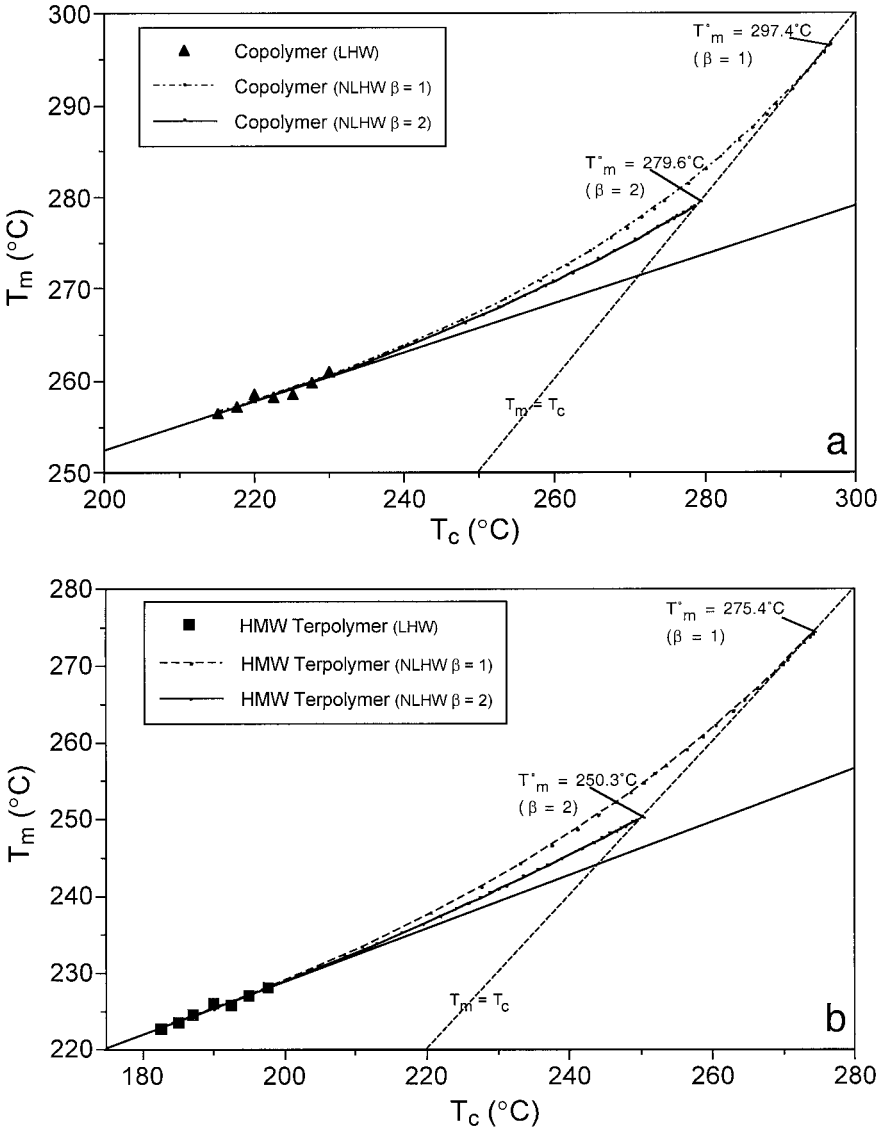

Figure 6 Hoffman–Weeks plot for the (a) copolymer and (b) terpolymer resins.

the Gibbs–Thomson analysis and likely greater than that obtained from the Hoffman–Weeks analysis for reasons already discussed. In what follows, we took the values to be 252.5°C for the HMW terpolymer and 249.5°C for the LMW terpolymer. However, it must be emphasized that the values for the terpolymers are only reasonable estimates based on our analysis of all the available data and errors. All things considered, we conclude that the estimated equilibrium melting temperature for the copolymer is likely to be fairly reliable. The values for the terpolymers are likely to be much less reliable and represent only reasonable approximations.

An estimate of the lateral surface free energy can be obtained from the modified Thomas–Staveley equation[21,29]:

$$\sigma = \alpha \Delta H_f \sqrt{a_0}\, b_0 \tag{3}$$

where α is the Thomas–Staveley constant; a_0, the width of the molecular stem; and b_0, the thickness of a layer of crystal being added at the growth front. The value of α for polyethylene has been shown to be 0.1. This value has often been assumed to be universal. While this is not the case, we believe that this is a good approximation for the present polyketones as their structure is quite

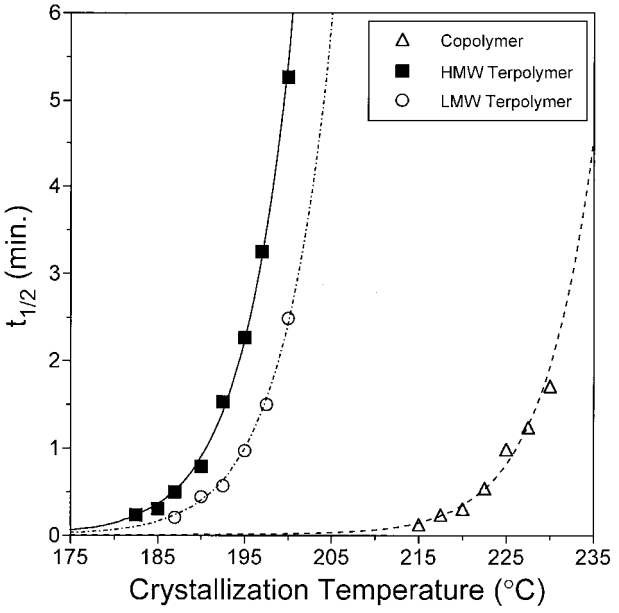

Figure 7 Isothermal crystallization half-times for the three resins.

similar to that of polyethylene. The values for a_0 and b_0 were calculated for the terpolymer and copolymer materials based on the β crystal structure, using the unit cell dimensions measured at elevated temperature by Klop et al.[12] Assuming that the (110) plane is the growth plane, the values a_0 = 4.74 Å and b_0 = 4.14 Å were obtained. This gives a value of 13.7 mJ/m^2 (numerically equivalent to ergs/cm^2) for the copolymer and 13.0 mJ/m^2 for the terpolymers for the lateral surface free energies. From the slope of the Gibbs–Thomson plots, the average values of the fold surface energies were estimated to be 56.5 mJ/m^2 for the copolymer. Since we have questioned the application of the Gibbs–Thomson analysis to the terpolymers, we will not compute the values of the fold surface free energy for the terpolymers from this technique.

Isothermal Crystallization Kinetics

Overall Crystallization Kinetics via DSC

Using the procedure outlined in the Experimental section, the crystallization half-time, $t_{1/2}$, of each resin was measured as a function of crystallization temperature. A plot of the half-times versus the crystallization temperature is shown in Figure 7. In this figure, each data point was determined from averages of runs made on fresh samples in order to keep the effects of the thermal history and crosslinking to a minimum.

An Avrami plot of representative data is shown in Figure 8. As indicated by the linear nature of this plot, the data followed the Avrami equation well. The Avrami exponents and rate constants were calculated from the slopes and intercepts of the Avrami plots; the results are presented in Table VI. The data generally show that the rate constant increases with a decrease in the temperature, as expected. The Avrami exponent lies in the range 2–3, in reasonable agreement with the earlier report.[14] While all the data shown in Table VI are from fresh samples, we did a few runs to examine the effects of the thermal history on the values of the Avrami exponents and rate constants. This was done by determining these quantities using data collected on the second and third repeat of the measurement using the same sample. These results showed that the increased thermal exposure caused a slight decrease in the Avrami exponents and probably also in the rate constant. This, presumably, results from the crosslinking that increases with the thermal exposure.

From the half-time and rate-constant results, it is observed that the LMW terpolymer material crystallizes slightly faster than does the HMW terpolymer material. Also, at a given temperature, the crystallization rate of the copolymer material is much higher than that of the other ma-

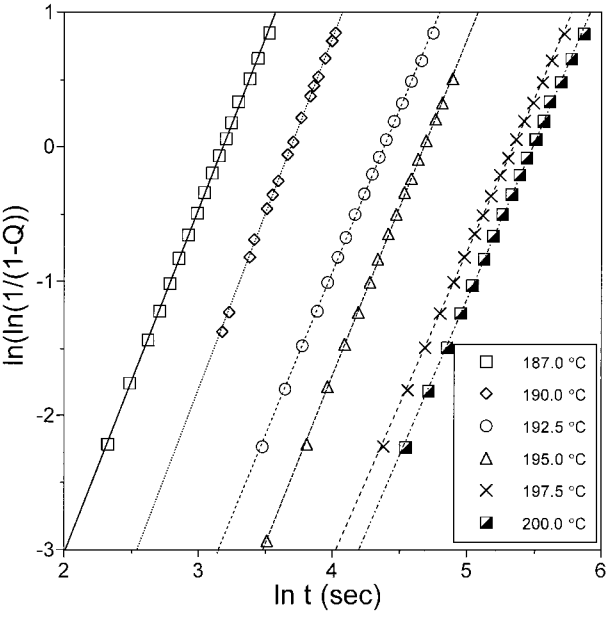

Figure 8 Avrami plot for the HMW terpolymer.

Table VI Avrami Exponent and Rate Constant Results

Material	T_c (°C)	Avrami Exponent	Rate Constant
HMW terpolymer	185.0	2.78	2.08×10^{-4}
	187.0	2.56	2.95×10^{-4}
	190.0	2.63	6.19×10^{-5}
	192.5	2.43	2.37×10^{-5}
	195.0	2.51	7.97×10^{-6}
	197.5	2.29	4.88×10^{-6}
	200.0	2.34	2.68×10^{-6}
LMW terpolymer	187.0	1.98	4.50×10^{-3}
	190.0	2.02	2.26×10^{-3}
	192.5	2.05	1.09×10^{-3}
	195.0	2.22	2.69×10^{-4}
	197.5	2.11	1.99×10^{-4}
	200.0	1.98	8.78×10^{-5}
Copolymer	217.5	2.09	2.70×10^{-3}
	220.0	2.28	2.97×10^{-3}
	222.5	2.55	2.08×10^{-4}
	225.0	2.85	8.89×10^{-6}
	227.5	2.15	8.27×10^{-5}
	230.0	2.16	4.68×10^{-5}

terials. This is presumably due to absence of structural defects that are present in the terpolymer. The defects presumably lower the rate at which the polymer chains are added to the crystal at the growth face. They also lower the equilibrium melting temperature, as shown earlier, leading to much greater supercooling below the equilibrium melting temperature at the accessible crystallization temperatures for the copolymer than for the terpolymer.

Linear Growth Rates

Due to the isothermal nature of the crystallization process, the spherulite radii were found to be linear with time at all crystallization temperatures up to the point at which significant spherulite impingement occurs. Thus, the spherulite growth rates, which are the slopes of the radius versus time curves, were constant at a given crystallization temperature. Figure 9 displays the relationship between the growth rate and the crystallization temperature for the polyketone materials. (It should be noted that the growth rate data could not be collected for crystallization temperatures above those given because significant degradation occurred before the crystallization process can be completed.) As expected, the growth rate increases as the crystallization temperature decreases. Figure 9 also shows that the growth rate values are higher for the copolymer than for the terpolymers at a given degree of undercooling, and for the terpolymer materials, the LMW material had slightly higher spherulite growth rate results than the those of the HMW material. This was expected since it is commonly found that an increase in molecular weight results in a decrease in the growth rates for unfractionated polymers.[30–32]

Hoffman–Lauritzen plots {$\log G + U^*/[2.3R(T_c - T_\infty)]$ versus $1/T\Delta Tf$} were constructed from linear growth rate data to calculate $\log G_0$ (G_0 is the growth rate constant) and K_g (nucleation constant) for the materials. The following values were assumed for the constants: $T_\infty = -20$°C and $U^* = 1500$ cal/mol. Figure 10 displays the Hoffman–Lauritzen plots for all three polyketones (the y-intercept equals $\log G_0$ and the slope is $-K_g/2.303$). A transition from regime III to II is clearly present in the copolymer and HMW terpolymer (crystallization temperature of approximately 224 and 203°C, respectively). The slopes of the two regions differ by a factor of two, which is consistent with regime theory. The LMW terpolymer seems to display this transition as well (crystallization temperature of approximately 200°C), but more data points in the regime II portion are required to be certain. It should be noted that the slopes of the two regions for the LMW terpolymer also differ by a factor of approximately two. The Hoffman–Lauritzen theory analyzes the growth data according to competition between the rate of deposition of secondary nuclei (**i**) and the rate of lateral surface spreading (**g**) resulting in three possible conditions. The theory suggests that regime II occurs when **i** and **g** are of the same order and is found under moderate supercooling, while regime III occurs when $\mathbf{i} > \mathbf{g}$ and is found under very high supercooling.

Figure 10 does not display much of a difference in K_g and $\log G_0$ for the terpolymers, while the value of K_g and $\log G_0$ for the copolymer is higher than that of the terpolymers (Table VII). Once K_g has been determined, other parameters characteristic of crystal growth can be calculated such as the lateral surface free energy (σ), fold surface free energy (σ_e), and the work of chain folding (q). The value of σ was calculated above and shown to be 13.7 mJ/m^2 for the copolymer and 13.0 mJ/m^2 for the terpolymers. The following equations were used to calculate σ_e and q:

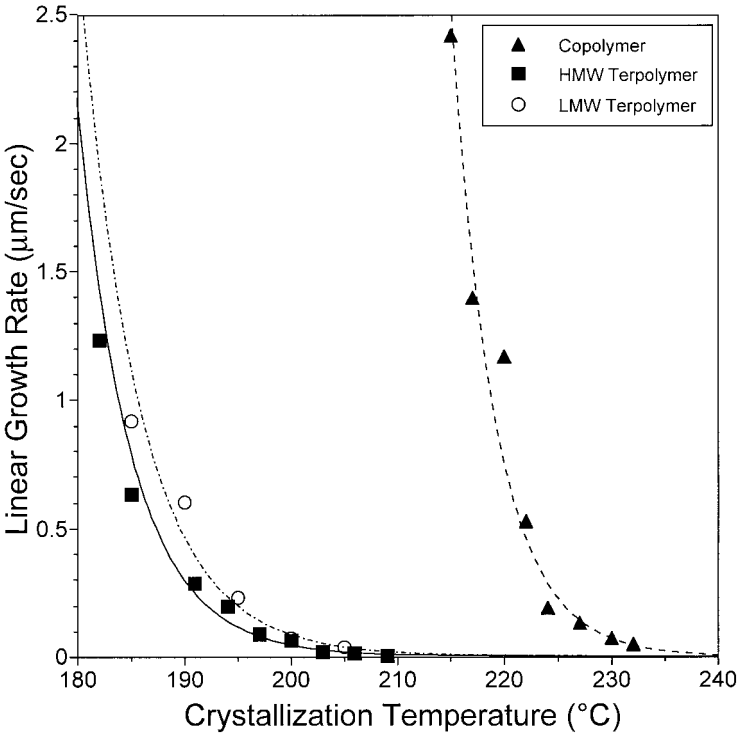

Figure 9 Linear growth rate versus crystallization temperature for the three resins.

$$K_g = \frac{jb_0\sigma\sigma_e T_m^0}{k\Delta h_f} \tag{4}$$

$$q = 2a_0b_0\sigma_e \tag{5}$$

where k is Boltzmann's constant and j is 4 for regimes I and III and 2 for regime II. The results for the terpolymers were again close, while the copolymer values were significantly higher (see Table VII). It is likely that this is due to the differences in the chemical and morphological structures of the materials. Perhaps the interface structure is very different for the terpolymer than for the copolymer. If we compare the results for the polyketones obtained by application of secondary nucleation theory to the results for polyethylene (σ = 14.1 erg/cm^2, σ_e = 90.4 erg/cm^2, and q = 5.0 kcal/mol from Hoffman et al.[21]), it is found that the σ_e value for polyethylene is lower than that of either the terpolymers or the copolymer. When compared to results for nylon 6,6 (σ = 8.0 erg/cm^2 and σ_e = 40.0 erg/cm^2 from Magill[33]), nylon 6,6 was found to have a σ_e value that is lower than that of either the terpolymers or the copolymer as well.

The fold surface free energy values calculated here from the growth kinetics are much higher than are the values obtained above from the Gibbs–Thomson equation (via SAXS). The value for σ_e calculated from the Gibbs–Thomson equation for the copolymer is slightly higher than the nylon 6,6 value but smaller than the polyethylene value. Other investigators found that the fold surface free energy values calculated from the thermodynamic method (Gibbs–Thomson) can differ significantly from the values obtained from growth rates (kinetic method). For example, Brown and Eby[34] obtained a value of 57 erg/cm^2 for σ_e for polyethylene using the Gibbs–Thomson approach, while, as described above, Hoffman et al.[21] obtained a value of 90.3 erg/cm^2 from analysis of the growth kinetics. There are four possible explanations for the observed differences between the values of σ_e obtained by the two different methods: In the first case, one can argue that the two values should not necessarily be the same since the two methods may not be measuring the same thing. The kinetic theory applies to the formation of the crystals during the crystallization process, while the equilibrium theory would seem to apply to established lamellae. Second, there are assumptions involved in both theories that may or may not be entirely valid in a given arbitrary system. The authors of the secondary nucle-

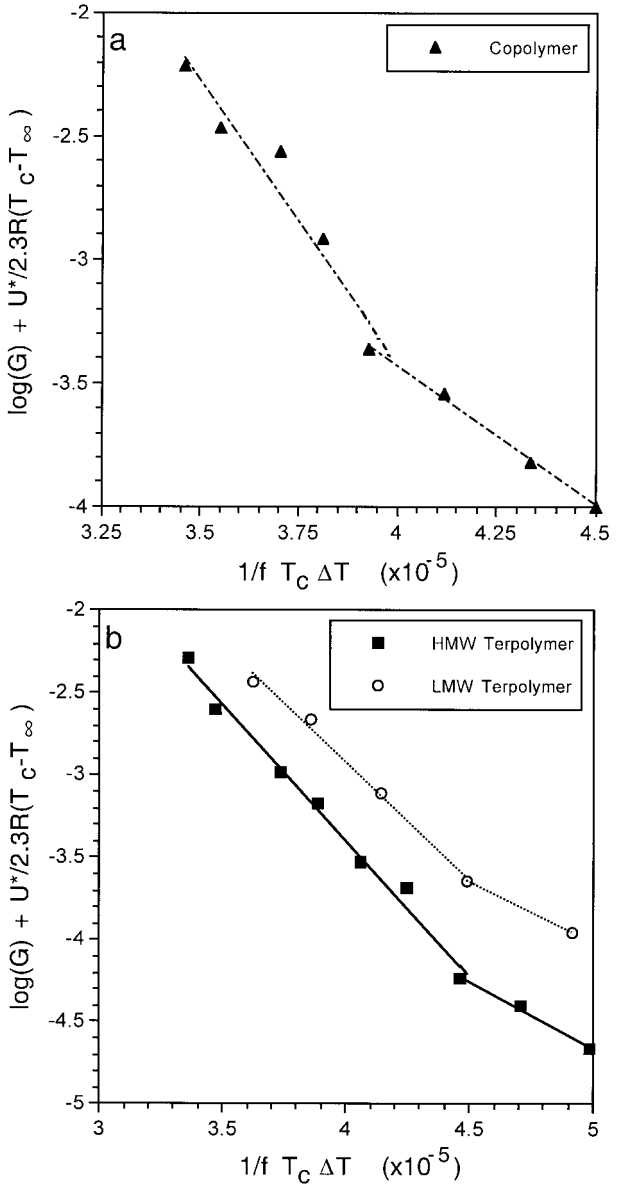

Figure 10 Hoffman–Lauritzen plots for the (a) copolymer and (b) terpolymer resins.

ation theory clearly indicated that the theory, as they have developed it, describes the behavior of polyethylene.[35] Although it is often used to describe the crystallization behavior of other polymers, it is not known how well it describes polymers in general. Also, in the case of the terpolymer, we should not forget the problems already discussed about the Gibbs–Thomson theory. Lastly, another possible explanation is that experimental errors may cause the differences. While we believe that we have done the best job we possibly could, under the circumstances, to obtain accurate data, some experimental error (perhaps substantial) is unavoidable due to the nature of the polymer system as we have described above. Hence, we offer the values of σ_e found here only as reasonable first approximations.

Nucleation

The Avrami exponent results from the DSC experiments suggest that the growth in the aliphatic polyketone materials is two- or three-dimensional and the nucleation is likely heterogeneous and instantaneous. While investigating the isothermal spherulite growth rates of these materials, it was noticed that, when multiple photomicrographs were taken at time intervals, the majority of the spherulites formed instantaneously while one or two additional spherulites appeared, in the field of view, about 0.03 s after the other spherulites had formed. All the spherulites would continue to grow at nearly identical growth rates. These observations seem to be consistent with heterogeneous, predetermined nucleation, which was suggested from the Avrami exponent results from the DSC experiments.

SUMMARY AND CONCLUSIONS

It was shown that the crosslinking reactions that occur in the aliphatic polyketones have a measurable effect on the thermal properties of these materials. For the grades studied, the effect causes a decrease of about 1° in the melting point and about 2 units (J/g) in the heat of fusion each time the material is melted within the suggested processing temperature range and then cooled. The latter result is presumably due to lower crystallinity with increase in the level of crosslinking. This behavior is typical of crosslinking materials.[36] When significant crosslinking occurs, it can also cause an increase in the time required for isothermal crystallization.

Wide-angle X-ray studies showed that crystallization of the terpolymer materials resulted largely in the β-phase which was retained at room temperature. Crystallization of the copolymer also produced the β-phase directly from the melt, but it was transformed to the α-phase on slow cooling to room temperature. No change in behavior was observed with a change in the crystallization temperature for any of the materials.

Table VII Parameters Derived from Kinetics Analysis of Aliphatic Polyketones

Material	K_g ($\times 10^5$) deg^2	log G_0	σ_e mJ/m^2 (erg/cm^2)	q (kcal/mol)	II–III Transition (°C)	II–III Supercooling (°C)
HMW terpolymer	1.89 (II)	−0.56 (II)	137.7 (II)	7.78 (II)		
	3.80 (III)	3.20 (III)	138.1 (III)	7.80 (III)	203	49
LMW terpolymer	1.68 (II)	−0.36 (II)	122.8 (II)	6.94 (II)		
	3.27 (III)	2.76 (III)	119.1 (III)	6.73 (III)	200	51
Copolymer	2.59 (II)	1.07 (II)	184.0 (II)	9.63 (II)		
	5.26 (III)	5.72 (III)	186.7 (III)	9.77 (III)	224	54

Optical microscopy showed that the polyketones exhibit a mixture of two types of spherulites classified on the basis of the sign of the birefringence: negative and mixed spherulites. The terpolymer materials seemed to have a higher number of the negative spherulites than did the copolymer; the latter had approximately equal numbers of negative and mixed spherulites.

Based on calculation from the measured heats of fusion of our samples and the crystallinity values measured from the density, the heat of fusion of the 100% crystalline copolymer (β-phase) was 239 ± 11 J/g. A similar calculation for the heat of fusion of the 100% crystalline terpolymer (β-phase) gave 226 ± 16 J/g.

SAXS studies showed that lamellae thickness increases with increasing crystallization temperature. The value of the lamellae thickness exhibited an approximately linear relationship with the temperature; values for both copolymer and terpolymer samples could be described by a single linear relationship.

Several techniques were used in an effort to determine the equilibrium melting temperatures of the present aliphatic polyketones. Using the lamellae thickness determined from the SAXS measurements, a Gibbs–Thomson plot produced the following equilibrium melting temperatures for the polyketone materials: 240°C for the HMW terpolymer, 238°C for the LMW terpolymer, and 278°C for the copolymer. The values determined from a Hoffman–Weeks plot were 244°C for the HMW terpolymer, 243°C for the LMW terpolymer, and 272°C for the copolymer. Values could not be determined from the nonlinear Hoffman–Weeks approach without an *a priori* assumption of the value of the lamella-thickening coefficient, β. With β assumed to be 2.0, the values obtained were 250.3°C for the HMW terpolymer, 249.5°C for the LMW terpolymer, and 279.6°C for the copolymer. If β is assumed to be 1.0, much higher values were obtained: 275.4, 273, and 297.4°C, respectively. An analysis based on spherulitic growth rates produced values of 252.5, 246, and 280°C, respectively. Based on these results, it was concluded that the most probable equilibrium melting temperature of the copolymer is 278 ± 2°C. The values for the terpolymers were too variable to establish conclusive values. After careful consideration, we chose 252°C for the HMW terpolymer and 249.5°C for the LMW terpolymer.

Crystallization studies carried out under isothermal conditions, using DSC, indicated that the copolymer crystallized faster than did the terpolymer materials, while the LMW terpolymer crystallized slightly faster than did the HMW terpolymer. Also, the Avrami exponent was found to lie in the range of 2–3, which is in reasonable agreement with an earlier report.[14]

Optical microscopy measurements of changes in the spherulite diameter with time showed the dependence of the crystal growth rates of these materials on the crystallization temperature. The growth rate values are higher for the copolymer than for the terpolymers at a given degree of undercooling. For the terpolymer materials, the LMW material had slightly higher spherulite growth rate results than those of the HMW material. Secondary nucleation theory was also used to determine regime III to regime II transitions and values for the nucleation constant (K_g), log G_0, the lateral surface free energy, the fold surface free energy, and the work of chain folding.

While investigating the isothermal spherulite growth rates of these materials, it was noticed that when multiple photomicrographs were taken at time intervals the great majority of the spheru-

lites formed instantaneously. This observation seems to be consistent with heterogeneous, predetermined nucleation, which was suggested from the Avrami exponent results from the DSC experiments. In future studies, we will investigate the structure and crystallization kinetics of aliphatic polyketones using several techniques that will concentrate on their behavior under nonisothermal conditions.

The authors wish to thank the Shell Chemical Co. for supplying the resins studied and for support of this research. The authors are particularly indebted to Dr. J. E. Flood for many discussions about the nature of the polyketone resins. The authors also thank Dr. J. S. Lin at the Center for Small Angle Scattering Research, Solid State Division, Oak Ridge National Laboratory, for help in obtaining and analyzing the SAXS data.

REFERENCES

1. Brubaker, M.; Coffman, D.; Hoehn, H. J Am Chem Soc 1952, 74, 1509.
2. Buback, M.; Tups, H. Physica B 1986, 139–140, 626.
3. Li, S. K. L.; Guillet, J. E. J Polym Sci: Polym Chem 1980, 18, 2221.
4. Gooden, R.; Hellman, M.; Simoff, D. A.; Winslow, F. New Trends in the Photochemmistry of Polymers; Elsevier: New York, 1985; Chapter 5, p 159.
5. Ward, R. M.; Kelley, D. C. Tappi J 1988, June, 140.
6. Drent, E. Eur. Patent Appl 121 965 A2, 1984; U.S. Patent 4 835 250, 1989.
7. Lommerts, B. J.; Klop, E. A.; Aerts, J. J Polym Sci Polym Phys Ed 1993, 31, 1319.
8. Starkweather, H. W., Jr. J Polym Sci Polym Phys 1977, 15, 247.
9. Chien, J. C. W.; Zhao A. X. Polym Degrad Stab 1993, 40, 257.
10. Chatani, Y.; Takizawa, T.; Murahashi, S.; Sakata, Y.; Nishimura, Y. J Polym Sci 1961, 55, 811.
11. Lommerts, B. J. Ph.D. Dissertation, University of Groningen, 1994.
12. Klop, E. A.; Lommerts, B. J.; Veurink, J.; Aerts, J.; Van Puijenbroek, R. R. J Polym Sci B Polym Phys 1995, 33, 315.
13. Ash, C. E.; Waters, D. G.; Smaardijk, A. A. In Annual Technical Conference Proceedings, XLI, Society of Plastics Engineers, Brookfield, CT, 1995; p 2319.
14. Flood, J. E.; Weinkauf, D. H.; Londa, M. In Annual Technical Conference Proceedings, XLI, Society of Plastics Engineers, Brookfield, CT, 1995; p 2326.
15. Machado, J. M.; Londa, M.; Verbeke, P.; Gergen W. P. In Annual Technical Conference Proceedings, XLI, Society of Plastics Engineers, Brookfield, CT, 1995; p 2335.
16. Weinkauf, D. H.; Kinneberg, P. A.; Ash, C. E. In Annual Technical Conference Proceedings, XLI, Society of Plastics Engineers, Brookfield, CT, 1995; p 2340.
17. Wignall, G.; Lin, J. S.; Spooner, S. J Appl Crystallogr 1990, 23, 241.
18. Wunderlich, B. Macromolecular Physics; Academic: New York, 1975; Vol. 1.
19. Haudin, J. M. In Optical Properties of Polymers; Meeren, G. H., Ed.; Elsevier: New York, 1983.
20. Hoffman, J. D.; Weeks, J. J Res Natl Bur Stand A 1962, 66, 13.
21. Hoffman, J. D.; Davis, G. T.; Lauritzen, J. I. In Treatise on Solid State Chemistry; Hannay, N .B., Ed.; Plenum: New York, 1976; Vol. 3.
22. Marand, H.; Xu, J.; Srinivas, S. Macromolecules 1998, 31, 8219.
23. Xu, J.; Srinivas, S.; Marand, H.; Agarwal, P. Macromolecules 1998, 31, 8230.
24. Alamo, R..; Viers, B.; Madelkern, L. Macromolecules 1995, 28, 3205.
25. De Rosa, C.; Auriemma, F.; Vinti, V.; Galimberti, M. Macromolecules 1998, 31, 6206.
26. Huang, J.; Prasad, A.; Marand, H. Polymer 1994, 35, 1896.
27. Flory, P. Principles of Polymer Chemistry; Cornell: New York, 1953.
28. Huggins, M. J Phys Chem 1942, 46, 151.
29. Thomas, D. G.; Staveley, L. A. K. J Chem Soc 1952, 4569.
30. Magill, J. H. J Polym Sci A 1969, 27, 1184.
31. Magill, J. H. J Polym Sci A 1967, 25, 89.
32. Magill, J. H. J Polym Sci 1964, 35, 3249.
33. Magill, J. H. Polymer 1965, 6, 367.
34. Brown, R. G.; Eby, R. K. J Appl Phys 1964, 35, 1156.
35. Hoffman, J. D.; Miller, R. L. Polymer 1997, 38, 3151.
36. Lambert, W. S.; Phillips, P. J. Polymer 1990, 31, 2007.